

**The in-plane paraconductivity in  
 $\text{La}_{2-x}\text{Sr}_x\text{CuO}_4$  thin film superconductors  
at high reduced-temperatures:  
Independence of the normal-state pseudogap**

Severiano R. Currás,<sup>1,2,\*</sup> Gonzalo Ferro,<sup>1</sup> M. Teresa González,<sup>1</sup>  
Manuel V. Ramallo,<sup>1</sup> Mauricio Ruibal,<sup>1</sup> José Antonio Veira,<sup>1</sup>  
Patrick Wagner,<sup>1,2,†</sup> and Félix Vidal<sup>1,‡</sup>

<sup>1</sup> LBTS,<sup>‡</sup> Departamento de Física da Materia Condensada,  
Universidade de Santiago de Compostela E15782, Spain.

<sup>2</sup> Laboratorium voor Vaste-Stoffysica en Magnetisme, Katholieke  
Universiteit Leuven, Celestijnenlaan 200 D, B3001 Heverlee, Belgium

## Abstract

The in-plane resistivity has been measured in  $\text{La}_{2-x}\text{Sr}_x\text{CuO}_4$  ( $\text{LS}x\text{CO}$ ) superconducting thin films of underdoped ( $x = 0.10, 0.12$ ), optimally-doped ( $x = 0.15$ ) and overdoped ( $x = 0.20, 0.25$ ) compositions. These films were grown on (100) $\text{SrTiO}_3$  substrates, and have about 150 nm thickness. The in-plane conductivity induced by superconducting fluctuations above the superconducting transition (the so-called in-plane paraconductivity,  $\Delta\sigma_{ab}$ ) was extracted from these data in the reduced-temperature range  $10^{-2} \lesssim \varepsilon \equiv \ln(T/T_C) \lesssim 1$ . Such a  $\Delta\sigma_{ab}(\varepsilon)$  was then analyzed in terms of the mean-field-like Gaussian-Ginzburg-Landau (GGL) approach extended to the high- $\varepsilon$  region by means of the introduction of a total-energy cutoff, which takes into account both the kinetic energy and the quantum localization energy of each fluctuating mode. The obtained GGL coherence length amplitude in the  $c$ -direction,  $\xi_c(0)$ , is constant for  $0.10 \leq x \leq 0.15$  [ $\xi_c(0) \simeq 0.9 \text{ \AA}$ ], and decreases with increasing  $x$  in the overdoped range [ $\xi_c(0) \simeq 0.5 \text{ \AA}$  for  $x = 0.20$  and  $\xi_c(0) \sim 0 \text{ \AA}$  for  $x = 0.25$ ]. These results strongly suggest, therefore, that the superconducting fluctuations in underdoped and overdoped  $\text{LS}x\text{CO}$  thin films may still be described, as in the optimally-doped cuprates, in terms of the extended GGL approach: The main effect of the doping is just to change the fluctuation dimensionality due to the change of the transversal superconducting coherence length amplitude. In contrast, the total-energy cutoff amplitude,  $\varepsilon^C$ , remains unchanged well within the experimental uncertainties. Our results strongly suggest that at all temperatures above  $T_C$ , including the high reduced-temperature region, the doping mainly affects in  $\text{LS}x\text{CO}$  thin films the normal-state properties and that its influence on the superconducting fluctuations is relatively moderate: Even in the high- $\varepsilon$  region, the in-plane paraconductivity is found to be independent of the opening of a pseudogap in the normal state of the underdoped films. We expect this last conclusion to be independent of the structural details of our films, *i.e.*, applicable also to bulk samples.

# 1 Introduction

It is now well established that some of the most central properties of the high-temperature cuprate superconductors (HTSC) strongly depend on the hole doping. [1] These properties include, *e.g.*, the normal-superconducting transition temperature,  $T_C$ , and also the opening of a pseudogap in the normal region in underdoped cuprates. Another property much affected by doping is the in-plane electrical conductivity parallel to the  $\text{CuO}_2$  planes,  $\sigma_{ab}$ , above the normal-superconducting transition. [1] It is also known that  $\sigma_{ab}$  in any HTSC is strongly affected around  $T_C$  by the presence of evanescent Cooper pairs created by thermal fluctuations (the so-called in-plane paraconductivity,  $\Delta\sigma_{ab}$ ). [2,3] In fact, these fluctuation effects may be appreciable even as far above  $T_C$  as  $T \simeq 1.5T_C$ . So,  $\sigma_{ab}$  may be decomposed as:

$$\sigma_{ab}(T, x) = \Delta\sigma_{ab}(T, x) + \sigma_{abB}(T, x), \quad (1)$$

where  $T$  is the temperature,  $x$  the hole doping level, and  $\sigma_{abB}(T, x)$  the so-called background or bare electrical in-plane conductivity (*i.e.*, the electrical in-plane conductivity if the fluctuations were absent). It is then natural to ask how much of the variation of  $\sigma_{ab}(T, x)$  observed when the doping is changed is due to  $\Delta\sigma_{ab}(T, x)$ , and how much to  $\sigma_{abB}(T, x)$ . In fact, once  $\sigma_{ab}(T, x)$  is measured, the above question is equivalent to ask how  $\Delta\sigma_{ab}(T, x)$  is affected by doping. This last question was first addressed by Suzuki and Hikita [4] and by Cooper and coworkers [5], and since then by different authors [6, 7, 8, 9, 10, 11, 12, 13, 14]. However, as of today some of the main conclusions (including, *e.g.*, the dimensionality of the fluctuations or the influence of the normal-state pseudogap) are still not well settled or they are even contradictory. For instance, in the case of  $\text{YBa}_2\text{Cu}_3\text{O}_x$  (YBCO $x$ ) some authors [5, 8, 13] proposed that  $\Delta\sigma_{ab}$  becomes more three-dimensional (3D) when  $x$  increases, whereas other authors [6, 11] did not find any appreciable dimensionality variation. Also, other authors have proposed, by analyzing either the fluctuation magnetization [14] or the thermal expansion [12], that the superconducting fluctuations in the underdoped YBCO $x$  do not follow the Gaussian mean-field-like theories used in Refs. [5, 6, 8, 11, 13] but follow instead different forms of non-Gaussian fluctuations. [12, 14] Another example of these discrepancies is provided by the studies of  $\text{La}_{2-x}\text{Sr}_x\text{CuO}_4$  (LS $x$ CO): By analyzing their measurements of the in-plane conductivity and magnetoconductivity, Suzuki and Hikita [4] proposed a change in dimensionality (2D to 3D) as doping increases from underdoped ( $x < 0.15$ ) to overdoped ( $x > 0.15$ ). In contrast, other authors [7] do not observe such a doping dependence in their magnetoresistance measurements in the same compounds. Let us stress here again that in addition to their interest for understanding the superconducting fluctuations in HTSC, the dependence of the paraconductivity on the doping may also concern other still open problems, as the origin of the pseudogap which opens in the normal state in the underdoped HTSC. [1] For instance, various theoretical models for such a pseudogap (see, *e.g.*, Refs. [15, 16, 17]) predict that the fluctuation effects would strongly vary with the doping level (even changing order of magnitude), while in

other models (see, *e.g.*, Refs. [18,19,20,21]) the pseudogap does not result in a change in the superconducting fluctuations.

Among the various possible reasons for the discrepancies commented above between the different studies of  $\Delta\sigma_{ab}(T, x)$ , four of them seem to be predominant: First, the different structural characteristics of the samples studied by each author (bulk or film samples, and in the latter case their thickness and substrate lattice parameters). In particular, as it is now well established, [22,23,24,25,26] the substrate effects (including the associated strain effects) change some of the properties of these thin films, such as the absolute values of their  $T_C$  and in-plane normal resistivity. The “*fine*” details of the paraconductivity, such as its dimensionality (which is directly related to the superconducting coherence length amplitude in the  $c$ -direction), may depend also on the structural nature of the samples. Let us stress already here, however, that it is also currently accepted that the most general aspects of the HTSC are similar for bulk and thin film samples. This is the case, in particular, of the evolution of  $T_C$  with doping or the appearance in the underdoped compositions of a pseudogap in the normal state. [1, 4, 5, 7, 23, 24, 26] Therefore, the conclusions concerning the relationships between superconducting fluctuations and pseudogap effects or the existence or not of indirect paraconductivity effects (see below) may be expected to be general, *i.e.*, independent of the structural characteristics of the superconductor. A second source of ambiguity is the probable presence in some of the samples of structural and stoichiometric inhomogeneities which, even when they are relatively small, may appreciably affect the measured  $\sigma_{ab}(T, x)$ , mainly near  $T_C$ . [27] Third, some authors [4,11] analyze their  $\Delta\sigma_{ab}(T, x)$  data in terms of the direct Aslamazov-Larkin (AL) contributions plus a pair-breaking (Maki-Thompson, MT) term, while others [6, 8, 9, 10, 13] take into account only the AL contributions, and yet others [5, 7] do not decide between both possibilities. Finally, a fourth source of ambiguity is that the region of reduced-temperatures,  $\varepsilon \equiv \ln(T/T_C)$ , where the data are analyzed was relatively small, typically  $10^{-2} \lesssim \varepsilon \lesssim 0.1$ , due to the fact that the conventional GGL approach is not applicable very near or very far away from  $T_C$ . [2, 3] To analyze the region  $\varepsilon \gtrsim 0.1$ , the usual mean-field-like theories have to be extended to deal with short-wavelength fluctuations, which above  $T_C$  become particularly important when  $\xi(T)$ , the superconducting coherence length, becomes of the order of  $\xi(0)$ , its amplitude extrapolated to  $T=0$  K. [2] Various attempts to study the paraconductivity in the high- $\varepsilon$  region as a function of doping in HTSC have been recently done by different authors. [9, 10, 13] In particular, Leridon *et al.* [13] analyzed the high- $\varepsilon$  paraconductivity in YBCO $x$  thin films with different dopings. Unfortunately, these authors based their analyses on a purely heuristic expression for the high- $\varepsilon$  paraconductivity, and the physical meaning of the involved parameters remains unclear. The high- $\varepsilon$  paraconductivity as a function of doping in Bi<sub>2</sub>Sr<sub>2</sub>CaCu<sub>2</sub>O<sub>8+x</sub> was studied by Asaka *et al.* [9] (using Ge-doped crystals) and by Silva *et al.* [10] (using oxygen-doped crystals but only in the overdoped range). These authors analyzed their data in terms of the GGL approach with the conventional kinetic energy (also called momentum) cutoff. Unfortunately, this conventional

cutoff [2] extends the applicability of the GGL paraconductivity only up to approximately  $\varepsilon \simeq 0.2$ . Both groups find that the cutoff parameter is doping-dependent, what is attributed by Asaka *et al.* to variations in the in-plane coherence length amplitude,  $\xi_{ab}(0)$ , and by Silva *et al.* to possible deviations from the BCS theory.

To further clarify the effects of doping near  $T_C$  on the superconducting fluctuations in HTSC, in this work we measure and analyze the in-plane paraconductivity of different high-quality  $LSxCO$  thin films with thickness around 150 nm, grown on (100)SrTiO<sub>3</sub> substrates and with Sr content corresponding to  $x = 0.10, 0.12, 0.15, 0.20$  and  $0.25$ . This kind of samples will allow us to compare even the “*fine*” details of the paraconductivity measured in our work with the measurements by Suzuki and Hikita [4], done in  $LSxCO$  films grown on the same substrate as ours and with thickness  $\sim 350$  nm. We also take advantage of three important aspects with respect to most of the previous works: First, the high controllability of the doping level in the  $LSxCO$  family has allowed us to grow  $c$ -axis oriented films with resistivities and transition widths among the best reported until now in this system. [1, 4, 23, 24, 26] Second, since the earlier results of Refs. [28, 29] it is today well established experimentally that the MT contributions to  $\Delta\sigma_{ab}$  are negligible in optimally-doped HTSC. This also agrees with the calculations in Refs. [30, 31] that indicate that for superconducting pairings with a  $d$ -wave component the strong pair-breaking effects of impurities make negligible the MT terms. It was also demonstrated experimentally the absence in the in-plane paraconductivity of optimally-doped HTSC of the so-called density-of-states (DOS) contributions. [29] So, in our analysis of the underdoped and overdoped  $LSxCO$  films we will assume the absence of appreciable indirect effects (MT and DOS). We are going to see here that such an assumption is well confirmed by our experimental results. A crucial advantage of our present work is to use recent extensions of the conventional mean-field-like calculations of  $\Delta\sigma_{ab}$  to the short-wavelength regime  $\varepsilon \gtrsim 0.1$ . [32, 33] These extensions are based on the introduction of a total-energy cutoff in the spectrum of the Gaussian-Ginzburg-Landau (GGL) superconducting fluctuations, accounting for the Heisenberg localization energy associated with the shrinkage, when the reduced-temperature increases, of the superconducting wave function. [34] These “extended” GGL expressions have already allowed us the analysis of the high- $\varepsilon$  in-plane paraconductivity of the optimally-doped  $YBCOx$ , [32] and more recently of the optimally-doped  $Bi_2Sr_2CaCu_2O_{8+x}$  and  $Tl_2Ba_2Ca_2Cu_3O_{10}$ . [33] The high- $\varepsilon$  paraconductivity in a single underdoped  $LSxCO$  film, with  $x \simeq 0.10$ , was also briefly analyzed in Ref. [33]. Note, however, that in such work the superconducting fluctuations were assumed to be essentially 2D. As we will see in the present work, this is not the most likely scenario for our underdoped  $LSxCO$  films in the  $\varepsilon \lesssim 0.1$  region. In analyzing our data, we will clearly emphasize what results are expected to be independent of the structural nature of the samples and which ones concern the “*fine*” behaviour of the paraconductivity and, therefore, are applicable only to thin films.

In Sect. II we describe the samples’ preparation and the resistivity measurements.

The extraction from these data of the in-plane paraconductivity, and their analysis in terms of the GGL model for superconducting fluctuations with a total-energy cut-off, is presented in Sect. III. We summarize our conclusions and discuss their main implications in Sect. IV.

## 2 Samples' preparation and electrical resistivity measurements

The samples studied in this work are *c*-axis-oriented  $LSxCO$  thin films grown on (100) $SrTiO_3$  substrates from ceramic single-targets with different Sr contents. All the films have similar thickness, of around 150 nm (see Table I). During deposition, by high-pressure DC sputtering with an on-axis cathode-substrate configuration, the substrate was held at temperatures between 840-860 °C in a flow of pure oxygen at 1.3 Torr. After deposition, the films were maintained during 30 minutes at the same temperature but at oxygen pressure of 7-10 Torr. Then, they were cooled down to room temperature to ensure full oxygenation. The crystal structure of the  $LSxCO$  films was studied by X-ray diffraction in a Bragg-Brentano geometry. The diffraction spectra exhibit only (00*l*) peaks, indicating then an oriented growth with the *c*-axis perpendicular to the substrate. The full-width at half-maximum of the rocking curve corresponding to the (006) reflection is around 0.3° for all the studied samples. Films were then patterned as narrow strips, with typical widths from 5 to 10  $\mu m$  and typical lengths of 100  $\mu m$ , by photolithography and wet chemical etching. Then, Au contact pads were deposited onto the current and voltage terminals, and annealed in oxygen at 1 atm and 600 °C during 15 minutes to facilitate gold diffusion into the  $LSxCO$ . The final resistance achieved was less than 0.1  $\Omega$  per contact. The in-plane resistivity of the films,  $\rho_{ab}(T)$ , was then measured by using a standard four-contact DC current arrangement in the temperature range from 4.2 K up to 300 K. The applied current was  $\sim 5 \mu A$ , which implies that the current density through the sample is around 100  $Acm^{-2}$  (much lower than the critical current density in zero applied magnetic field). The resolutions in the  $\rho_{ab}(T)$  measurement are about 1  $\mu\Omega cm$  for resistivity, and about 10 mK for temperature.

In Figs. 1 to 3 it is shown the temperature-dependence of  $\rho_{ab}(T)$  for our  $LSxCO$  thin films, with Sr contents  $x=0.10, 0.12, 0.15, 0.20$  and  $0.25$ . These  $x$  values are the ones given by the nominal deposition rates. As it can be seen in these figures, upon increasing the Sr content the in-plane resistivity decreases gradually and its  $T$ -dependence well above  $T_C$  changes systematically from a concave shape (for  $x \leq 0.15$ ) to a more linear one (for  $x > 0.15$ ). Such a doping-dependence of the resistivity is in good agreement with previous results in similar  $LSxCO$  films. [1, 4, 23, 24, 26, 33] For all the films studied here, the values of  $\rho_{ab}$  at 250 K (see Table I) are among the lowest

reported until now in the literature for films with the same doping and substrate and similar thickness. [1, 4, 23, 24, 26, 33] Another indication of the quality of our samples is the width of the superconducting transition in the  $\rho_{ab}(T)$  curves, which are also among the smallest in the literature. In Fig. 3 it is shown the detail of  $\rho_{ab}(T)$  around the superconducting transition and the corresponding  $d\rho_{ab}/dT$ . In this figure it is also shown  $T_{CI}$ , the temperature where  $d\rho_{ab}/dT$  reaches its maximum, and  $T_{CI}^-$  and  $T_{CI}^+$ , corresponding to the half-maximum of such a derivative peak above and, respectively, below  $T_{CI}$ . The value of  $T_{CI}$ ,  $T_{CI}^-$  and  $T_{CI}^+$  for all the samples studied in this work is given in Table I. Also, in Fig. 4 we show the  $T_{CI}$  values of our films as a function of Sr content. As it can be easily seen in such figure,  $T_{CI}$  rises with increasing the Sr content up to a optimal doping level of about  $x = 0.15$ , and then decreases. These  $T_{CI}$  values, and also their doping dependence, are in good agreement with the ones at present well established for  $T_C$  in  $LSxCO$  films with similar substrate and thickness (note that the  $T_{CI}$  values of good-quality bulk  $LSxCO$  are higher than in thin films with similar Sr content, although both types of samples share the same  $T_{CI}$  dependence on doping). [1, 4, 23, 24, 26, 33] In the remaining of this work we will use, unless specified otherwise,  $T_{CI}$  as  $T_C$ . The appropriateness of such a choice in the analysis of the in-plane paraconductivity will be discussed in further detail in subsection 3.4.

### 3 The in-plane paraconductivity: Comparison with the extended GGL approach

#### 3.1 Extraction of the in-plane paraconductivity

As usually, [2,3]  $\Delta\sigma_{ab}$  is obtained from the measured  $\rho_{ab}(T)$  curves by just using Eq.(1) and estimating the normal-state background  $\rho_{abB}$  (*i.e.*,  $\sigma_{abB}^{-1}$ ) by extrapolating through the transition the  $\rho_{ab}(T)$  data measured well above the region where  $\Delta\sigma_{ab}(\varepsilon)$  is to be analyzed. As we want to analyze  $\Delta\sigma_{ab}(\varepsilon)$  also in the high- $\varepsilon$  ( $\varepsilon > 0.1$ ) region, we will use a procedure similar to the one already used in Refs. [32,33]. This is a two-step process: First, we fit the  $\rho_{ab}(T)$  data in the  $T$ -region  $1.6T_C \lesssim T \lesssim 2.7T_C$  (corresponding to  $0.5 \lesssim \varepsilon \lesssim 1$ ). To perform such a fit, we used the simplest functionality producing good agreement with the data at all dopings, which is a linear plus a Curie-like term,  $a/T + b + cT$ . Indeed, such a background is appropriate to analyze  $\Delta\sigma_{ab}(\varepsilon)$  only well below  $\varepsilon \simeq 0.5$ . And, in fact, similar types of extrapolations have been successfully used to obtain  $\Delta\sigma_{ab}(\varepsilon)$  up to  $\varepsilon \simeq 0.1$  in various optimally-doped HTSC (see, *e.g.*, Refs. [3,28,29,35]). Now then, by construction this background makes  $\Delta\sigma_{ab}$  to become zero at  $\varepsilon = 0.5$ , and thus cannot lead to a trustworthy  $\Delta\sigma_{ab}(\varepsilon)$  analysis for the high- $\varepsilon$  ( $\varepsilon > 0.1$ ) region. So, the second step to determine a background valid for our purposes will be to fit the  $\rho_{ab}(T)$  data at considerably higher reduced-temperatures, in the  $T$ -range  $4.5T_C \lesssim T \lesssim 7T_C$  (which corresponds to  $1.5 \lesssim \varepsilon \lesssim 2$ ). However, because the

extrapolation uncertainties strongly increase with the  $T$ -distance, we require to this last fit to reproduce in the moderate- $\varepsilon$  range  $10^{-2} \lesssim \varepsilon \lesssim 0.1$  the  $\Delta\sigma_{ab}(\varepsilon)$  results obtained with our first background estimate, up to a  $\pm 20\%$  maximum uncertainty. We used for these fits a Curie-like plus a 2nd.-degree polynomial term,  $a/T + b + cT + dT^2$ , which is the simplest functional producing in the enlarged  $T$ -region good fits for all  $x$ . A detailed account of the uncertainty associated with our background estimation, mainly focused on its impact on our analyses of  $\Delta\sigma_{ab}(\varepsilon)$ , will be presented later in subsection 3.4. However, let us emphasize already here that such backgrounds do not appreciably depend on variations of the lower limit of the background fitting region,  $T_B^L$ , from its default value  $4.5T_C$ , provided that  $T_B^L$  is kept above  $\sim 3.5T_C$  (*i.e.*, above  $\varepsilon \simeq 1.2$ ). In Figs. 1 to 3 we plot the normal-state backgrounds obtained by using the above procedure in all the films studied in this work. Note that the upwards concavity of  $\rho_{abB}(T)$  diminishes for  $x \geq 0.15$ . Also shown in Figs. 1 and 2 is  $T^C$ , the temperature at which  $\Delta\sigma_{ab}(\varepsilon)$  is observed to become negligible. We emphasize that  $T^C$  is well below  $T_B^L$ , and also that there is few variation of  $T^C$  when  $T_B^L$  is moved, always if  $T_B^L \gtrsim 3.5T_C$  (see also subsection 3.4). This indicates that the existence of such a  $T^C$  is not an artifact of the background subtraction procedure.

In Fig. 5 we show the  $\Delta\sigma_{ab}$ -versus- $\varepsilon$  curves obtained for each of the films measured in this work. This figure already illustrates a result central in our present paper: The experimental  $\Delta\sigma_{ab}(\varepsilon)$  curves agree with each other well within the experimental errors for the doping levels  $0.10 \leq x \leq 0.15$  (corresponding to the underdoped and optimally-doped range of compositions). Note that this conclusion does not rely on any comparison with any theory. This striking result already suggests the non-validity, at least for  $LSxCO$  films, of the proposals by various authors (see, *e.g.*, Refs. [1, 12, 14, 15, 16, 17]) that the superconducting fluctuations are substantially different in underdoped and optimally-doped HTSC. As also shown in Fig. 5, in the overdoped range of compositions (*i.e.*, for  $x = 0.20$  and  $0.25$ ) the in-plane paraconductivity of the  $LSxCO$  films increases with the value of  $x$ , mainly in the  $\varepsilon$ -region  $\varepsilon \lesssim 0.1$ . At higher reduced-temperatures, all the  $\Delta\sigma_{ab}(\varepsilon)$  curves (for all  $x$ ) collapse towards negligible paraconductivity at a reduced-temperature  $\varepsilon$  of around 0.8.

## 3.2 Theoretical background: Extension of the GGL paraconductivity to the high- $\varepsilon$ region

To analyze the experimental data summarized in the above subsection, we will use the paraconductivity expressions obtained on the grounds of the mean-field GGL approach regularized through the so-called “total-energy” cutoff, which takes into account the limits imposed by the uncertainty principle to the shrinkage of the superconducting wave function when the temperature increases well above  $T_C$ . [34] Our results in optimally-doped HTSC suggest that such a regularization extends the applicability of

the mean-field-like GGL approach from the  $\varepsilon_{\text{LG}} \lesssim \varepsilon \lesssim 0.1$  region to the high- $\varepsilon$  region. [32, 33, 34] Here  $\varepsilon_{\text{LG}}$  is the so-called Levanyuk-Ginzburg reduced-temperature, below which the fluctuations enter in the full-critical, non-Gaussian region where non-mean-field approaches (like the 3DXY model) must be applied. [36] Such an  $\varepsilon_{\text{LG}}$  was estimated to be of the order of  $10^{-2}$  in HTSC. [3, 36] Note also that so close to  $T_C$  the effects of sample inhomogeneities may considerably affect the paraconductivity data. [27] Therefore, in the present paper we will restrict our analyses to the mean-field-like  $\varepsilon \gtrsim 10^{-2}$  region. Although the GGL in-plane paraconductivity under the total-energy cutoff was calculated for the first time in Ref. [32], it will be useful to summarize in this subsection some of the results of such calculations for the case of single-layered superconductors, and also remember the physical meaning of the total-energy cutoff, which was analyzed in terms of the uncertainty principle applied to the superconducting wave function in Ref. [34]. For layered superconductors with a single interlayer separation,  $s$  (the case of the  $\text{LSxCO}$  family, where  $s = 6.6 \text{ \AA}$ ), the total-energy cutoff may be written as:

$$k_{xy}^2 + \frac{B_{\text{LD}}(1 - \cos(k_z s))}{2\xi_{ab}^2(0)} + \xi_{ab}^{-2}(\varepsilon) \leq \xi_{ab0}^{-2}. \quad (2)$$

In this expression,  $\mathbf{k}_{xy}$  and  $\mathbf{k}_z$  are the in-plane and  $c$ -direction wavevectors of the fluctuating modes,  $\xi_{ab}(\varepsilon) = \xi_{ab}(0)\varepsilon^{-1/2}$  is the in-plane GL coherence length,  $B_{\text{LD}} \equiv (2\xi_c(0)/s)^2$  is the so-called Lawrence-Doniach (LD) dimensional crossover parameter,  $\xi_{ab}(0)$  and  $\xi_c(0)$  are the in-plane and, respectively, out-of-plane GL superconducting coherence length amplitudes, and  $\xi_{ab0}$  is the in-plane Pippard coherence length. Note that  $\mathbf{k}_z$  is limited by the layered structure as  $-\pi/s \leq k_z \leq \pi/s$ .

The left-hand side in Eq.(2) is the total energy of a fluctuation mode (in units of  $\hbar^2/2m_{ab}^*$ , where  $\hbar$  is the reduced Plank constant and  $m_{ab}^*$  is the in-plane effective mass of the superconducting pairs). As explained in Ref. [34], this ‘‘total-energy’’ of each fluctuation mode may be seen as the sum of the Heisenberg localization energy associated with the shrinkage of the superconducting wave function when the temperature increases above  $T_C$  [the  $\xi_{ab}^{-2}(\varepsilon)$  term] and the conventional kinetic energy. In the case of single-layered superconductors, the kinetic energy appears as the sum of two contributions: The in-plane kinetic energy (the  $k_{xy}^2$  term) and the  $c$ -direction kinetic energy savings [the  $B_{\text{LD}}(1 - \cos(k_z s))/2\xi_{ab}^2(0)$  term]. The right-hand side in Eq.(2) may be seen as the localization energy associated to the maximum shrinkage, at  $T = 0 \text{ K}$ , of the superconducting wave function. This term is, therefore, proportional to the inverse square of the in-plane Pippard coherence length amplitude,  $\xi_{ab0}$  (see Ref. [34]).

To briefly analyze the differences between the total-energy cutoff and the conventional momentum or kinetic-energy cutoff, the simplest case is the 2D layered limit, where  $B_{\text{LD}} = 0$ . In that case Eq.(2) simplifies to:

$$k_{xy}^2 + \xi_{ab}^{-2}(\varepsilon) \leq \xi_{ab0}^{-2}. \quad (3)$$

Near  $T_C$ , when  $\xi_{ab}(\varepsilon) \gg \xi_{ab0}$ , the localization energy contribution to each fluctuation mode may be neglected, and Eq.(3) reduces then to the conventional momentum or kinetic-energy cutoff in 2D layered superconductors: [2]

$$k_{xy}^2 \leq c \xi_{ab}^{-2}(0). \quad (4)$$

where instead of the Pippard  $\xi_{ab0}$  we have used  $c^{-1/2}\xi_{ab}(0)$ , where  $c$  is a cutoff amplitude, temperature-independent, close to 1. These expressions still simplify in the case of isotropic 3D superconductors: The total-energy cutoff reduces to  $k^2 + \xi^{-2}(\varepsilon) \leq \xi_0^{-2}$ , whereas one refinds  $k^2 \leq c \xi^{-2}(0)$  for the momentum or kinetic-energy cutoff, which is the familiar condition earlier proposed for low- $T_C$  superconductors. [2] By using again  $\xi_0 = c^{-1/2}\xi(0)$  and assuming the applicability at all reduced-temperatures of the mean-field  $\varepsilon$ -dependence of the superconducting coherence length,  $\xi(\varepsilon) = \xi(0)\varepsilon^{-1/2}$ , one may see that the conventional kinetic-energy and the total-energy cutoffs are related, in the 2D and 3D limits, through the substitution of  $c$  by  $c - \varepsilon$ . So, as stressed before both cutoffs coincide near  $T_C$ , when  $\varepsilon \ll c$ . The conventional momentum or kinetic-energy cutoff appears then as a particular case, the limit when  $\xi(\varepsilon) \gg \xi_0$ , of the total-energy cutoff. However, in spite of the simple relationship between both cutoff approaches, first proposed in Ref. [37], their deep conceptual differences also lead to striking differences in the high- $\varepsilon$  behaviour of any observable associated with the superconducting fluctuations above  $T_C$ , included the paraconductivity. These differences have been analyzed in Refs. [32,33,34], but it could be useful to stress here some of them. Note first that the maximum in-plane kinetic energy of the fluctuating Cooper pairs,  $E_{ab,kinetic}^{\max}$ , is temperature-independent in the case of the conventional kinetic-energy or momentum cutoff. For instance, for 2D layered superconductors,

$$E_{ab,kinetic}^{\max}(\text{momentum cutoff}) = \frac{(\hbar k_{xy}^{\max})^2}{2m_{ab}^*} = \frac{\hbar^2}{2m_{ab}^* \xi_{ab}^2(0)} c. \quad (5)$$

In contrast, under a total-energy cutoff the maximum in-plane kinetic energy of the Cooper pairs is temperature-dependent. In this example (2D layered superconductors), the corresponding  $E_{ab,kinetic}^{\max}$  may be directly obtained from Eq.(5) by using  $c - \varepsilon$  instead of  $c$  [or from Eq.(3) and using again  $\xi_{ab0} = c^{-1/2} \xi_{ab}(0)$  and  $\xi_{ab}(\varepsilon) = \xi_{ab}(0)\varepsilon^{-1/2}$ ] as:

$$E_{ab,kinetic}^{\max}(\text{total-energy cutoff}) = \frac{\hbar^2}{2m_{ab}^* \xi_{ab}^2(0)} (c - \varepsilon), \quad \text{with } \varepsilon \leq c, \quad (6)$$

which is temperature-dependent and that becomes zero for  $\varepsilon \geq c$ . In other words, in contrast with the conventional momentum or kinetic-energy cutoff which only eliminates, independently of the temperature, the fluctuating modes with in-plane kinetic energy above  $c\hbar^2/2m_{ab}^*\xi_{ab}^2(0)$ , the total-energy cutoff eliminates *all* the fluctuation modes at reduced-temperatures equal to  $c$  or above. By imposing a zero kinetic-energy in Eqs. (2) or (3), this reduced-temperature, denoted  $\varepsilon^C$ , is given by:

$$\xi_{ab}(\varepsilon^C) = \xi_{ab0}, \quad (7)$$

*i.e.*,  $\varepsilon^C = (\xi_{ab}(0)/\xi_{ab0})^2$ . As first argued in Ref. [34], Eq.(6) (which leads directly to the existence of a well-defined reduced-temperature above which all coherent Cooper pairs vanish) may be seen as just a consequence of the limitations imposed by the uncertainty principle to the shrinkage of the superconducting wave function, which also above  $T_C$  imposes the condition  $\xi_{ab}(\varepsilon) \geq \xi_{ab0}$ : In other words, the collective behaviour of the Cooper pairs will be dominated at high reduced-temperatures by the Heisenberg localization energy. [34] If, in addition, we assume the applicability of the BCS relationship in the clean limit,  $\xi_{ab}(0) = 0.74\xi_{ab0}$ , then  $\varepsilon_{\text{BCSclean}}^C = c_{\text{BCSclean}} \simeq 0.6$ . [33, 34, 38] Indeed this value of  $c$  will also apply to the conventional momentum cutoff approach that appears as the limit when  $\varepsilon \ll 1$  of the total-energy cutoff.

As we are particularly interested in analyzing the dimensionality of the superconducting fluctuations in  $\text{LSxCO}$  as a function of the doping, we will first summarize here the general expressions of the paraconductivity as a function of the LD dimensional crossover parameter,  $B_{\text{LD}}$ . Then we will also present the limiting cases  $B_{\text{LD}} \ll \varepsilon$  (2D limit) and  $B_{\text{LD}} \gg \varepsilon$  (3D limit). The paraconductivity for single-layered superconductors resulting from the GGL approach extended to high reduced-temperatures by the total-energy cutoff has been calculated in Ref. [32] to be:

$$\Delta\sigma_{ab}(\varepsilon)_{\text{E}} = \frac{e^2}{16\hbar s} \left[ \frac{1}{\varepsilon} \left( 1 + \frac{B_{\text{LD}}}{\varepsilon} \right)^{-1/2} - \frac{1}{\varepsilon^C} \left( 2 - \frac{\varepsilon + B_{\text{LD}}/2}{\varepsilon^C} \right) \right], \quad (8)$$

where  $e$  is the electron's charge. The paraconductivity under a total-energy cutoff in the 2D limit may be then obtained by just applying in Eq. (8) the condition  $B_{\text{LD}} \ll \varepsilon$ : [32]

$$\Delta\sigma_{ab}^{2\text{D}}(\varepsilon)_{\text{E}} = \frac{e^2}{16\hbar s} \left[ \frac{1}{\varepsilon} - \frac{1}{\varepsilon^C} \left( 2 - \frac{\varepsilon}{\varepsilon^C} \right) \right]. \quad (9)$$

Concerning the paraconductivity under a total-energy cutoff in the 3D limit, it cannot be directly obtained from Eq.(8) because this equation assumes the  $c$ -direction layered-structure cutoff,  $-\pi/s \leq k_z \leq \pi/s$ , which in the limit  $B_{\text{LD}} \gg \varepsilon$  is no longer a stronger limitation for  $k_z$  than the total-energy cutoff [Eq.(2)]. [32] The calculations using the total-energy cutoff for the three directions of space have been also done in Ref. [32], the resulting expression being:

$$\Delta\sigma_{ab}^{3\text{D}}(\varepsilon)_{\text{E}} = \frac{e^2}{48\pi\hbar\xi(0)} \left\{ 3 \left[ \frac{\arctan(\sqrt{(\varepsilon^C - \varepsilon)/\varepsilon})}{\sqrt{\varepsilon}} - \frac{\varepsilon\sqrt{\varepsilon^C - \varepsilon}}{(\varepsilon^C)^2} \right] - 5 \frac{(\varepsilon^C - \varepsilon)^{3/2}}{(\varepsilon^C)^2} \right\}. \quad (10)$$

Let us also summarize the results for the in-plane paraconductivity under the conventional momentum cutoff. As first explicitly derived by Asaka *et al.* [9] (see also Ref. [32] for a more detailed calculation), the corresponding expression for a single-layered superconductor is:

$$\Delta\sigma_{ab}(\varepsilon)_{\text{M}} = \frac{e^2}{16\hbar s} \left\{ \frac{1}{\varepsilon} \left( 1 + \frac{B_{\text{LD}}}{\varepsilon} \right)^{-1/2} \frac{c(c + \varepsilon + B_{\text{LD}}/2)}{[(c + \varepsilon + B_{\text{LD}})(c + \varepsilon)]^{3/2}} - \frac{1}{\varepsilon + c} \left( 1 + \frac{B_{\text{LD}}}{\varepsilon + c} \right)^{-1/2} \right\}. \quad (11)$$

The corresponding results in the 2D and 3D limits are, respectively:

$$\Delta\sigma_{ab}^{2D}(\varepsilon)_M = \frac{e^2}{16\hbar s} \left[ \frac{1}{\varepsilon} - \frac{c}{(c+\varepsilon)^2} - \frac{1}{\varepsilon+c} \right], \quad (12)$$

and

$$\Delta\sigma_{ab}^{3D}(\varepsilon)_M = \frac{e^2}{48\pi\hbar\xi(0)} \left\{ 3 \left[ \frac{\arctan(\sqrt{c/\varepsilon})}{\sqrt{\varepsilon}} - \frac{\varepsilon\sqrt{c}}{(\varepsilon+c)^2} \right] - 5 \frac{c^{3/2}}{(\varepsilon+c)^2} \right\}. \quad (13)$$

Equations (12) and (13) correspond to the expressions first obtained for these 2D and 3D limits by Gauzzi and Pavuna in Ref. [35]. It is also useful to note here the differences between the asymptotic behaviour of  $\Delta\sigma_{ab}(\varepsilon)$  under the two different cutoff conditions. For instance, as it is well known, [32, 35] in the 2D limit the conventional momentum cutoff predicts that  $\Delta\sigma_{ab}^{2D}(\varepsilon)_M$  smoothly decays as  $\varepsilon^{-3}$  when  $\varepsilon \gg c$ . In contrast, as stressed before, the paraconductivity under a total-energy cutoff presents a singularity when  $\varepsilon = \varepsilon^C = c$ . Such a behaviour is not describable through a critical exponent in  $\varepsilon$ . However, when  $\varepsilon$  approaches  $c$  from below such a singular behaviour may be described in terms of a power law in  $|\tilde{\varepsilon}|$ , where  $\tilde{\varepsilon} \equiv \varepsilon - c$ . In the 2D limit, this asymptotic behaviour is:

$$\Delta\sigma_{ab}^{2D}(\tilde{\varepsilon})_E = \frac{e^2}{16\hbar s c^3} |\tilde{\varepsilon}|^2, \quad \text{for } \tilde{\varepsilon} \rightarrow 0^-. \quad (14)$$

The in-plane paraconductivity without any cutoff may be directly obtained from the above  $\Delta\sigma_{ab}(\varepsilon)$  expressions by just imposing  $\varepsilon \ll \varepsilon^C$  in Eqs.(8) to (10) [or  $\varepsilon \ll c$  in Eqs.(11) to (13)]. This leads to the well-known Lawrence-Doniach expression for a single-layered superconductor:

$$\Delta\sigma_{ab}(\varepsilon)_{\text{no cutoff}} = \frac{e^2}{16\hbar s} \frac{1}{\varepsilon} \left( 1 + \frac{B_{LD}}{\varepsilon} \right)^{-1/2}, \quad (15)$$

which recovers in the limits  $B_{LD} \ll \varepsilon$  and  $B_{LD} \gg \varepsilon$  the also well-known results by Aslamazov and Larkin for the paraconductivity without any cutoff in 2D and 3D superconductors:

$$\Delta\sigma_{ab}^{2D}(\varepsilon)_{\text{no cutoff}} = \frac{e^2}{16\hbar s \varepsilon}, \quad (16)$$

and

$$\Delta\sigma_{ab}^{3D}(\varepsilon)_{\text{no cutoff}} = \frac{e^2}{32\hbar\xi_c(0)} \varepsilon^{-1/2}. \quad (17)$$

Finally, let us stress here that all the above expressions for the in-plane paraconductivity [Eqs.(8) to (17)] implicitly assume a relaxation time for the superconducting fluctuations equal to the one given by the standard BCS mean-field approach,  $\tau_0 = (\pi\hbar/8k_B T_C)\varepsilon^{-1}$ . [39] They also consider that all indirect contributions (as the Maki-Thompson and the density-of-states ones) to  $\Delta\sigma_{ab}(\varepsilon)$  are negligible, as it is today well established for the HTSC. [28, 29]

### 3.3 Comparison between the experimental data and the GGL paraconductivity

We present in Fig. 5 a comparison between the theoretical in-plane paraconductivity under a total-energy cutoff and the experimental data obtained in the different LS $x$ CO films measured in this work. The solid lines in these figures are the best fits of Eq.(8) to the experimental data in all the measured  $\varepsilon$ -region. In these fits, we have used  $T_{CI}$  as  $T_C$ , the only free parameters being  $\xi_c(0)$  and  $\varepsilon^C$ . The so-obtained values for  $\xi_c(0)$  and  $\varepsilon^C$  are summarized in Table I. The error bars and the  $x$ -dependence of these values will be discussed later in detail. As it is easily observable in this Fig. 5, the agreement between Eq.(8) and the experimental data is excellent in all the region  $10^{-2} \lesssim \varepsilon \lesssim 1$ , for all the samples studied in this work. This comparison confirms, in particular, the existence of a well-defined reduced-temperature,  $\varepsilon^C$ , of about  $\varepsilon^C \sim 0.8$ , above which the in-plane paraconductivity vanishes. A different view of these fits is provided by Figs. 2 and 3. In these figures, the continuous lines are the theoretical  $\rho_{ab}(T)$  curves which result from the above analyses [*i.e.*, from adding, through Eq.(1), the normal-state background and the theoretical  $\Delta\sigma_{ab}(\varepsilon)$  resulting from the above fits]. As visible in these figures, the agreement with the  $\rho_{ab}(T)$  measurements above the transition is again excellent.

It may be useful to check if the GGL theory with a total-energy cutoff may also explain the in-plane resistivity measurements done by Suzuki and Hikita [4] in their own LS $x$ CO films, with various  $x$  values, grown on the same substrate as ours, and with thickness  $\sim 350$  nm. For that, we have scanned the corresponding published  $\rho_{ab}(T)$  plots [4] and applied to these data the same analysis as described above. Some examples of the so-obtained  $\Delta\sigma_{ab}(\varepsilon)$  curves, and their comparison with Eq.(8), are shown in Fig. 6. As it is evident in this figure, the GGL approach with a total-energy cutoff also explains these measurements, again in the  $10^{-2} \lesssim \varepsilon \lesssim 1$  range. These data also confirm the existence of a well-defined reduced-temperature,  $\varepsilon^C$ , above which the in-plane paraconductivity vanishes. We emphasize that in performing these analyses we have again used  $T_{CI}$  as  $T_C$ , and not included any Maki-Thompson (MT) indirect contribution to the in-plane paraconductivity (which, as commented in the Introduction, are now well established to be absent in the HTSC [28, 29]). As noted before, Suzuki and Hikita assumed in their analyses the existence of such MT contribution. In fact, to be able to introduce the MT contribution, Suzuki and Hikita had to consider the critical temperature as an additional adjustable parameter. This led to  $T_C$ 's appreciably different from  $T_{CI}$ . Our present analysis of the data of Suzuki and Hikita also indicates that the in-plane paraconductivity in LS $x$ CO films grown in (100)SrTiO<sub>3</sub> substrates is, as it could be expected, almost independent of thickness in the range 150 – 350 nm. However, let us stress again that using bulk samples, or films grown on different substrates or with significantly different thickness, may change some of the fine details of the paraconductivity, as in particular the corresponding  $\xi_c(0)$  values (see also below).

In Fig. 7 we show the comparison between the experimental  $\Delta\sigma_{ab}(\varepsilon)$  measured in the present work and the paraconductivity expressions without any cutoff and under the conventional momentum or kinetic-energy cutoff, using the same values for  $\xi_c(0)$  and  $\varepsilon^C$  as in Fig. 5. This figure evidences that, as it could be expected, the momentum or kinetic-energy cutoff expressions are able to fit the experimental paraconductivity in a lower  $\varepsilon$ -range than the total-energy cutoff (up to at most  $\varepsilon \simeq 0.3$  for the momentum cutoff, and up to about  $\varepsilon \simeq 0.1$  for no cutoff). In particular, they fail to reproduce the rapid fall-off of the fluctuations in the higher- $\varepsilon$  region,  $\varepsilon \gtrsim 0.3$ .

Let us now discuss the doping-dependence of the parameters  $\xi_c(0)$  and  $\varepsilon^C$  which results from the above fits using the GGL approach under a total-energy cutoff. In Fig. 8 we show such  $\xi_c(0)$  and  $\varepsilon^C$  values as a function of the doping. Let us first remark the trend for the variations of  $\xi_c(0)$  with the doping level  $x$ : For  $x \leq 0.15$ , *i.e.*, in the underdoped and optimally-doped range,  $\xi_c(0)$  is found to be approximately equal to  $0.9 \text{ \AA}$ . This value corresponds to a LD dimensional crossover parameter  $B_{LD} \simeq 7.5 \times 10^{-2}$ . For  $x = 0.20$  it is  $\xi_c(0) \simeq 0.5 \text{ \AA}$  (and hence  $B_{LD} \simeq 2 \times 10^{-2}$ ), and for  $x \simeq 0.25$  and above it is  $\xi_c(0) \sim 0 \text{ \AA}$  (so  $B_{LD} \sim 0$  and the fluctuations are 2D in all the studied  $\varepsilon$ -range). This  $\xi_c(0)$ -versus- $x$  trend is consequent with our observation that the fluctuation conductivity is the same for the underdoped and optimally-doped LS $x$ CO films, and increases with  $x$  in the overdoped ones. Let us also note that in Refs. [23,24,25] it has been argued that the substrate may induce in LS $x$ CO films  $c$ -direction stress, what in turn may change the interlayer tunneling. Therefore, LS $x$ CO films grown on different substrates or with significant different film thickness, and also LS $x$ CO bulk samples, may have  $\xi_c(0)$  values different to the ones found in the present work. In this regard, we have found through measurements of the fluctuation-induced magnetization that the superconducting fluctuations are bidimensional in underdoped *bulk* LS $x$ CO samples, in contrast with our present results for thin films. [40] It has been also found in Refs. [41,42] that the superconducting bidimensionality is smeared or suppressed in the overdoped bulk samples of the LS $x$ CO family. The comparison of these observations with our present results suggests then that the substrate effects in LS $x$ CO films do affect  $\xi_c(0)$ , and therefore the interlayer tunneling of Cooper pairs.

Concerning the other free parameter in our  $\Delta\sigma_{ab}(\varepsilon)$  fits,  $\varepsilon^C$ , we find that its value remains the same within the experimental uncertainties for all the studied LS $x$ CO films (see Fig. 8 and Table I). Such a value, which taking into account its experimental uncertainty (mainly associated with the background subtraction, see below) is bounded by  $0.4 \lesssim \varepsilon^C \lesssim 1.1$ , is in fair agreement with the value  $\sim 0.6$  that may be crudely estimated on the grounds of the mean-field  $\varepsilon$ -dependence of  $\xi_{ab}(\varepsilon)$  and the BCS value of  $\xi_{ab}(0)/\xi_{ab0}$  in the clean limit (see subsection 3.2 and Ref. [34]). We note that the validity of such a simple estimate has been also confirmed, usually with a lower error band, by the analysis of the superconducting fluctuations in various optimally-doped HTSC and various clean and moderately dirty LTSC (see Ref. [34] and references therein). We note also that our previous analyses of the fluctuation magnetization in

a bulk underdoped LSxCO led to  $\varepsilon^C \simeq 0.6 \pm 0.2$ . This is consistent with the fact that, as already mentioned in subsection 3.2 and further elaborated in Ref. [34], the appearance of the reduced-temperature cutoff  $\varepsilon^C$  is expected to occur in all superconductors independently of, *e.g.*, their structural character or of the dimensionality of the superconducting fluctuations.

### 3.4 On the influence of the background and $T_C$ choices

It is of relevance to discuss in detail the main sources of uncertainties in the above analyses of the experimental paraconductivity in terms of the extended GGL approach. Let us first consider the uncertainties associated with the extraction of the normal-state background contribution,  $\rho_{abB}(T)$ . As already mentioned, we have checked that varying the lower limit of the background fitting region from its value in our analyses,  $T_B^L = 4.5T_C$ , does not significantly change the obtained  $\Delta\sigma_{ab}(\varepsilon)$  curves, provided that  $T_B^L$  is kept above  $\sim 3.5T_C$  (otherwise it would force the paraconductivity to become negligible at progressively lower reduced-temperatures, therefore affecting  $T^C$  and  $\varepsilon^C$ ). Adding a 3rd. degree polynomial term to the background functionality does not appreciably change the paraconductivity curves that we have obtained. We have also checked that using a variable-range-hopping contribution,  $\rho_1 \exp(T_0/T)^{1/4}$ , instead of the  $b/T$  term (as proposed, *e.g.*, by Leridon and coworkers [13] when analyzing the high- $\varepsilon$  paraconductivity of YBCO $x$  films) does not change the obtained backgrounds, within a maximum of 2% variation. The more appreciable source of uncertainty in the background subtraction comes from its freedom to deviate  $\pm 20\%$  at  $10^{-2} \lesssim \varepsilon \lesssim 0.1$  from the  $\Delta\sigma_{ab}$  obtained with the background fitted closer to the transition (fitted in the  $T$ -region  $1.6T_C \lesssim T \lesssim 2.7T_C$ , *i.e.*,  $0.5 \lesssim \varepsilon \lesssim 1$ ). The  $\pm 20\%$  figure was chosen after verifying that it is a good measure of the variations of such “low- $\varepsilon$  background” when its fitting region is somewhat varied. While this uncertainty has relatively low impact on the  $\Delta\sigma_{ab}(\varepsilon)$  curves for  $10^{-2} \lesssim \varepsilon \lesssim 0.1$ , its influence becomes stronger in the high reduced-temperature region ( $\varepsilon > 0.1$ ), affecting mainly the precise value of  $\varepsilon^C$  (or, equivalently, of  $T^C$ ). In particular, lower backgrounds indeed lead to lower  $\varepsilon^C$  and  $T^C$ . However, let us emphasize that this uncertainty does not affect the qualitative shape of the sharp fall-off of  $\Delta\sigma_{ab}$  at high reduced-temperatures, but only the precise location of such a fall-off. In Fig. 9 we illustrate the uncertainty of the  $\Delta\sigma_{ab}(\varepsilon)$  curves associated to the choice of the background. The limits of the shaded areas correspond to the lower and higher backgrounds obtained for each sample. This figure clearly illustrates that the background uncertainty does not affect the low- $\varepsilon$  region in a dramatic way, and therefore its impact on the value of  $\xi_c(0)$  is also moderate. Table I summarizes the corresponding  $\varepsilon^C$  and  $\xi_c(0)$  uncertainty for all the LSxCO films measured in this work.

It may be also useful to study the influence of the  $T_C$  choice in our analyses. First of all, we note that the  $d\rho_{ab}/dT$  peaks around  $T_{CI}$  present about 1 K of half-widths at

half-maximum of the peak (see Fig. 3 and Table I). Taking into account the relatively low critical temperature of the  $LSxCO$  family, such widths correspond to rather high reduced-temperatures, of the order of  $\varepsilon \sim 5 \times 10^{-2}$ . This means that varying  $T_C$  inside the upper half of the  $T_{CI}$  peak may considerably affect the paraconductivity versus reduced-temperature curves in a sizable  $\varepsilon$ -region of our  $\Delta\sigma_{ab}(\varepsilon)$  fits. Such uncertainty is illustrated in Fig. 10 for the cases  $x = 0.10$  and  $0.25$ : In this figure, the same  $\Delta\sigma_{ab}$  data as in Fig. 5 is plotted against  $\varepsilon \equiv \ln(T/T_C)$  for  $T_C$  values in between  $T_{CI}^-$  and  $T_{CI}^+$  (the lower and upper temperature boundaries of the  $T_{CI}$  peak at half-maximum). Also plotted is Eq.(8) in those cases where it is possible to find  $\xi_c(0)$  and  $\varepsilon^C$  values producing a valid agreement with such  $\Delta\sigma_{ab}(\varepsilon)$  data curves. As it is clearly illustrated by the figure, using  $T_C$ 's below  $T_{CI}$  makes  $\Delta\sigma_{ab}(\varepsilon)$  to increase, and  $T_C$ 's above  $T_{CI}$  makes  $\Delta\sigma_{ab}(\varepsilon)$  to decrease. In the case  $x = 0.10$ , when lowering  $T_C$  it is possible to fit Eq.(8) up to  $T_C$  values  $T_C = T_{CI} - 0.6K$  ( $=T_{CI}^-+0.2K$ ). This is accomplished by lowering  $\xi_c(0)$ , while the parameter  $\varepsilon^C$  remains almost unchanged from  $\varepsilon^C=0.8$ . In fact, using  $T_C = T_{CI} - 0.6K$  leads to a fit with already  $\xi_c(0) = 0 \text{ \AA}$ ; because of this, with lower  $T_C$ 's Eq.(8) can no longer account for the data. In the case of the  $x = 0.25$  film, however,  $\xi_c(0) = 0 \text{ \AA}$  already corresponds to  $T_C=T_{CI}$  and hence the  $\Delta\sigma_{ab}(\varepsilon)$  curves cannot be successfully fitted by Eq.(8) if using any  $T_C$  below  $T_{CI}$ . Let us now discuss what happens when using  $T_C$ 's above  $T_{CI}$  instead of below. In such a case, the  $\Delta\sigma_{ab}(\varepsilon)$  curves decrease. Such a decrease can be to some extent reproduced by Eq.(8), for all the doping levels, by increasing  $\xi_c(0)$  and slightly changing also  $\varepsilon^C$ . However, as shown in Fig. 10, the resulting fits are always of somewhat inferior quality than when using  $T_{CI}$ . To sum up, using  $T_{CI}$  as  $T_C$  seems to be the best choice because of the consistency when taking into account the data of films with different doping levels, and because it provides better-quality fits than  $T_C$ 's taken above  $T_{CI}$ . However, we think that it is useful to bear in mind the conclusion that relatively small deviations from  $T_{CI}$  will have an appreciable impact on the values of  $\xi_c(0)$ . In particular, the  $\xi_c(0)$  values obtained for each  $LSxCO$  film using  $T_{CI}^+$  instead of  $T_{CI}$  are  $1.8 \text{ \AA}$  for  $x = 0.10$ ,  $2.0 \text{ \AA}$  for  $x = 0.12$ ,  $1.9 \text{ \AA}$  for  $x = 0.15$ ,  $1.6 \text{ \AA}$  for  $x = 0.20$ , and  $1.5 \text{ \AA}$  for  $x = 0.25$ . Also, for all the doping levels studied here it is possible to find a  $T_C$  in between  $T_{CI}^-$  and  $T_{CI}$  leading to  $\xi_c(0) \simeq 0 \text{ \AA}$ . In fact, such uncertainties accumulate to the reasons commented in the Introduction to explain the discrepancies between different authors when proposing values for  $\xi_c(0)$  from the analysis of the superconducting fluctuations in  $LSxCO$ . For instance, in our previous work [33] we briefly analyzed a single  $LSxCO$  film, with  $x = 0.10$ , assuming  $\xi_c(0) \simeq 0 \text{ \AA}$ , what leded us to conclude that  $T_C$  was nearer to  $T_{CI}^-$  than to  $T_{CI}$ . Finally, let us emphasize here that when using in our present analyses any choice of  $T_C$  with similar displacements with respect to  $T_{CI}$  for all the  $x$ -values it remains true our main qualitative conclusions: The paraconductivity is constant with  $x$  in the underdoped and optimally-doped  $LSxCO$  thin films, but increases with  $x$  in the overdoped range up to  $x \simeq 0.25$ . Also, the choice of  $T_C$  does not affect the fact that the fluctuations sharply decrease at a well-defined reduced-temperature well above  $T_C$ .

## 4 Concluding remarks

In this paper we have presented measurements of the in-plane paraconductivity  $\Delta\sigma_{ab}$  above the superconducting transition of various high-quality  $LSxCO$  thin films with thickness  $\sim 150$  nm grown on (100) $SrTiO_3$  substrates, with doping levels  $x$  varying from 0.10 to 0.25, in the reduced-temperature range  $10^{-2} \lesssim \varepsilon \lesssim 1$ . Our results confirm, and extend to high reduced-temperatures, the earlier proposals by Suzuki and Hikita [4] and by Cooper and coworkers [5] that in HTSC the variations of  $\Delta\sigma_{ab}$  with doping may explain only a small part of the variations of the total in-plane conductivity  $\sigma_{ab}$  near  $T_C$ . In fact, for the under- and optimally-doped compositions our results directly show that the corresponding  $\rho_{ab}(T)$  varies appreciably whereas the  $\Delta\sigma_{ab}(\varepsilon)$  curves agree with each other well within the experimental uncertainties. Our results also show that in the overdoped regime  $\Delta\sigma_{ab}(\varepsilon)$  increases only moderately with  $x$ . The absence of important anomalous doping effects on the paraconductivity is confirmed by the fact that our  $\Delta\sigma_{ab}(\varepsilon)$  data may be appropriately accounted for by the Gaussian-Ginzburg-Landau (GGL) approach, extended to the high- $\varepsilon$  region ( $\varepsilon \gtrsim 0.1$ ) by means of a total-energy cutoff. The fits using such an approach lead to  $c$ -direction superconducting coherence length amplitudes,  $\xi_c(0)$ , of about 0.9 Å for the under- and optimally-doped films, about 0.5 Å for the  $x = 0.20$  overdoped film, and  $\xi_c(0)$  negligibly small ( $\sim 0$  Å) for the  $x = 0.25$  one. Moreover, independently of the doping, we observe in all these  $LSxCO$  films a rapid decrease of the superconducting fluctuation effects in the high- $\varepsilon$  region. Such a decrease is also well explained by the GGL approach with a total-energy cutoff, which takes into account the quantum localization energy associated with the limits imposed by the uncertainty principle to the shrinkage of the superconducting wave function as  $\varepsilon$  increases. [34]

In what concerns the fine behaviour of the in-plane paraconductivity with doping, our results also confirm the proposal by Suzuki and Hikita [4] that in  $LSxCO$  films the main effect of doping on the superconducting fluctuations is to change the  $c$ -direction superconducting coherence length,  $\xi_c(0)$ . However, because of the use of MT terms in their analyses, these authors concluded that  $\xi_c(0)$  would increase as  $x$  increases in the under-, optimally-, and over-doped regimes. In contrast, we have shown here that when such terms are considered to be negligible one obtains a different doping dependence of  $\xi_c(0)$ , as summarized above. As the absence of MT and DOS contributions to the in-plane paraconductivity is at present well established, [28, 29] we believe that the true behaviour of  $\xi_c(0)$  with doping in  $LSxCO$  thin films grown in (100) $SrTiO_3$  substrates is probably the one we propose here. Let us also note that the dependence of  $\xi_c(0)$  with doping found here in  $LSxCO$  films may be not applicable to  $LSxCO$  bulk samples, as the substrate may also change  $\xi_c(0)$  and, therefore, the dimensionality of the superconducting fluctuations. In particular, it has been found in Ref. [40], through measurements of the fluctuation-induced magnetization, that the superconducting fluctuations are bidimensional in underdoped *bulk*  $LSxCO$  samples, in contrast with our

present results for thin films. It has been also found in Refs. [41,42] that the superconducting bidimensionality is smeared or suppressed in the overdoped bulk samples of the  $LSxCO$  family. These differences between thin films and bulk samples of  $LSxCO$  seem to be due to strain effects associated with the grown on a substrate with  $ab$ -plane lattice constants different to those of bulk  $LSxCO$ . [22, 23, 24, 25] Proposals that the main effect of doping on the superconducting fluctuations is to change  $\xi_c(0)$  were also done (and almost simultaneously to Suzuki and Hikita [4]) for the  $YBCOx$  compound by Cooper *et al.* [5] (and later also by Juang *et al.* [8]). We note however that our present results cannot be directly extrapolated to  $YBCOx$  because in this compound doping happens in the interlayer CuO-chains, absent in  $LSxCO$ . Such CuO-chains are expected to determine most of the interlayer tunneling in  $YBCOx$  due to their metallic-like character. Another central result of our analyses is that the cutoff parameter,  $\varepsilon^C$ , arising in the “extended” GGL approach is found to be, well within the experimental uncertainties, independent of the doping. As the conventional momentum cutoff is just a particular case, valid for  $\varepsilon \lesssim 0.2$ , of the total-energy cutoff approach, our conclusion will then apply to any analysis in terms of such a momentum cutoff. This suggests, therefore, that the doping dependence of the momentum cutoff observed in other HTSC compounds (see, *e.g.*, Refs. [9] and [10]) could be an extrinsic effect due to the presence of sample inhomogeneities or to ambiguities in the background estimate.

Our results may also have implications on other open problems of the HTSC. First of all, they allow us to conclude, as mentioned in the title of this paper, that the superconducting fluctuations in underdoped  $LSxCO$  films are not linked to the opening of their normal-state pseudogap: First, because the variations of doping in such underdoped compounds, which are known to vary the pseudogap opening temperature,  $T^*$ , [1] do not result in any observable change of the superconducting fluctuations, even in the high- $\varepsilon$  region. Second, because also in such underdoped compositions the superconducting fluctuations have been found here to disappear at reduced-temperatures which are, even taken into account the experimental uncertainties, always below 1.1, *i.e.*, much below  $T^*$  (that is located above room temperature for the underdoped compositions studied in this work [1]). In other words, our experimental results seem to be contradictory with the theoretical proposals that in HTSC the superconducting fluctuations are strongly enhanced when underdoping. [1, 12, 14, 15, 16, 17] Such proposals include, *e.g.*, the ones that the pseudogap effects observed in the underdoped HTSC are due to strong fluctuations of the superconducting order parameter (and in particular of its phase), which in turn would be due to either a Bose-Einstein-like preformation of Cooper pairs [15], stripe-like inhomogeneities [14, 17], or bidimensionality effects [16]. For instance, in Ref. [15] it is claimed that the superconducting fluctuations in underdoped HTSC will be given essentially by the 2D-Kosterlitz-Thouless model of fluctuations [43] with relaxation times of such fluctuations various orders of magnitude bigger than the BCS mean-field one implied by Eq.(8). However, our present analyses strongly suggest that there is no change in the order of magnitude of the superconducting fluctuations when the doping level enters the underdoped range.

There is also no evidence in our experimental data of any dependence on  $x$  of the critical exponents of  $\Delta\sigma_{ab}(\varepsilon)$  for  $0.10 \leq x \leq 0.15$ . Our results favor then the theoretical proposals associating the pseudogap opening to purely normal-state effects (as, *e.g.*, those of Refs. [18, 19, 20]), or the theories where the Bose-Einstein preformed pairs are dressed by normal quasiparticles [21]. In those approaches, consistently with our present results, the superconducting order parameter is expected to undergo Gaussian, mean-field-like fluctuations, except in the very close vicinity of  $T_C$  (for  $\varepsilon \lesssim 10^{-2}$ ). It would be useful to determine whether other proposals for the doping effects in HTSC, such as the existence of a  $T = 0$  K quantum transition near optimal doping, [44] would lead to Gaussian or non-Gaussian superconducting fluctuations above  $T_C$ .

The results presented here may also have implications on the theoretical proposals by Horbach and coworkers [45] for the paraconductivity in the marginal-Fermi-liquid (MFL) scenario, which would apply to the optimally-doped and overdoped HTSC. According to the calculations in Ref. [45], the inelastic scattering of normal quasiparticles in optimally-doped and overdoped HTSC would decrease the relaxation time of the superconducting fluctuations below the BCS mean-field value, and correspondingly also  $\Delta\sigma_{ab}$ . Horbach and coworkers estimate such changes in  $\Delta\sigma_{ab}$  to be of the order of a prefactor 0.2-0.75 (depending mainly on a cut parameter affecting their numerical evaluations). [45] However, our present results indicate that the relaxation time of the superconducting fluctuations takes the BCS mean-field value for all the doping levels. They also indicate that  $\Delta\sigma_{ab}$  is not smaller in the optimally-doped and overdoped films than it is in the underdoped films [in fact, it is even higher in the overdoped films because of their lower  $\xi_c(0)$ ].

It may be also useful to compare our results for the  $\xi_c(0)$  dependence on doping with detailed measurements of the normal-state anisotropy in  $LSxCO$  films. For instance, in Ref. [46] it is measured the resistivity in  $LSxCO$  thin films grown with the  $c$ -axis oriented obliquely with respect to the substrate. From such measurements, it was proposed that the normal-state anisotropy decreases as doping increases. If confirmed by different measurements, this would indicate that the interlayer tunneling of the normal and superconducting carriers would not be directly related. This could be coherent, *e.g.*, with the interlayer tunneling model for the superconducting condensation in HTSC proposed by Anderson and coworkers. [20] Further work to compare the normal and superconducting interlayer tunnelings in  $LSxCO$  films is clearly needed, both theoretical and experimental (for instance, through measurements of the intrinsic interlayer Josephson effects and of the normal and superconducting magnetoconductivity). Further work is also needed to study the possible influence on the “*fine*” details of the superconducting fluctuations of the film thickness and of the type of substrate. As mentioned previously, both factors are known to vary several crucial properties of the  $LSxCO$  films, like their  $T_C$  and  $\rho_{ab}(250\text{ K})$  values, possibly due in part to strain effects associated with the grown on a substrate with  $ab$ -plane lattice constants different to those of bulk  $LSxCO$ . [1, 4, 7, 22, 23, 24, 25, 26] In the present paper we have

found a transversal superconducting coherence length for  $LSxCO$  films which is different, both in value and doping dependence, to the one that seems to arise from Ref. [40] (where the fluctuation magnetization in a bulk underdoped  $LSxCO$  was measured) and Refs. [41, 42] (where the superconducting anisotropy of  $LSxCO$  bulk samples with different dopings was measured). It would be interesting, therefore, to further study the relationships between sample thickness, type of substrate, and superconducting interlayer tunnelings [or, equivalently,  $\xi_c(0)$ ].

This work has been supported by the CICYT, Spain, under grants no. MAT2001-3272 and MAT2001-3053, by the Xunta de Galicia under grant PGIDT01PXI20609PR, and by Unión Fenosa under grant 0666-2002.

## References

- \* Present address: Low Temperature Division, Department of Applied Physics and MESA+ Research Institute, University of Twente, P.O. Box 217, 7500 AE Enschede, The Netherlands.
  - † Present address: Institute for Materials Research, Limburgs Universitair Centrum, Wetenschapspark 1, B-3590 Diepenbeek, Belgium.
  - ‡ Corresponding author. E-mail: [fmvidal@usc.es](mailto:fmvidal@usc.es)
  - ‡ Laboratorio de Baixas Temperaturas e Supercondutividade (Unidad Asociada al Instituto de Ciencias de Materiales de Madrid, Consejo Superior de Investigaciones Científicas, Spain).
- [1] For a detailed review of the doping effects in cuprates see, *e.g.*, T. Timusk and B. Statt, Rep. Progr. Phys. **62**, 61 (1999). See also, V.M. Loktev, R.M. Quick, and S.G. Sharapov, Phys. Rep. **349**, 1 (2001). For a summary centered in  $LSxCO$ , see, *e.g.*, P.G. Radaelli, D.G. Hinks, A.W. Mitchell, B.A. Hunter, J.L. Wagner, B. Dabrowski, K.G. Vandervoort, H.K. Viswanathan, and J.D. Jorgensen, Phys. Rev. B **49**, 4163 (1994).
- [2] The general aspects of the superconducting fluctuations in low- and high- $T_C$  superconductors may be seen, *e.g.*, in M. Tinkham, *Introduction to Superconductivity* (McGraw-Hill, New York) 1996, ch. 8; W.J. Skocpol and M. Tinkham, Rep. Prog. Phys. **38**, 1049 (1975).

- [3] For a summary of the paraconductivity in optimally-doped HTSC and earlier references see, *e.g.*, F. Vidal and M.V. Ramallo, in *The gap symmetry and fluctuations in high- $T_C$  superconductors*, ed. J. Bok, G. Deutscher, D. Pavuna, and S.A. Wolf (NATO-ASI series, Plenum), 1998, p. 443.
- [4] M. Suzuki and M. Hikita, Phys. Rev. B **44**, 249 (1991); Phys. Rev. B **47**, 2913 (1993).
- [5] J.R. Cooper, S.D. Obertelli, A. Carrington, and J.W. Loram, Phys. Rev. B **44**, 12086 (1991); A. Carrington, D.J.C. Walker, A. P. Mackenzie, and J.R. Cooper, Phys. Rev. B **48**, 13051 (1993).
- [6] N. Mori, Y. Takano, H. Enomoto, H. Ozaki, and K. Sekizawa, Physica B **194-196**, 2049 (1994).
- [7] T. Kimura, S. Miyasaka, H. Takagi, K. Tamasaku, H. Eisaki, S. Uchida, K. Kitazawa, M. Hiroi, M. Sera, and N. Kobayashi, Phys. Rev. B **53**, 8733 (1996).
- [8] J.Y. Juang, M.C. Hsieh, C.W. Luo, T.M. Uen, K.H. Wu, and Y.S. Gou, Physica C **329**, 45 (2000).
- [9] K. Asaka, K. Koizumi, H. Bando, N. Mori, H. Ozaki, Physica B **284-288** 995 (2000).
- [10] E. Silva, S. Sarti, R. Fastampa, and M. Giura, Phys. Rev. B **64**, 144508 (2001).
- [11] A. Gueffaf, M. Salim, and M.S. Raven, J. Phys: Condens. Matter **13**, 875 (2001).
- [12] C. Meingast, V. Pasler, P. Nagel, A. Rykov, S. Tajima, and P. Olsson, Phys. Rev. Lett. **86**, 1606 (2001).
- [13] B. Leridon, A. Défossez, J. Dumont, J. Lesueur, and J.P. Contour, Phys. Rev. Lett. **87**, 197007 (2001).
- [14] P. Carretta, A. Lascialfari, A. Rigamonti, A. Rosso, and A. Varlamov, Phys. Rev. B **61**, 12420 (2000); A. Lascialfari, A. Rigamonti, L. Romano, P. Tedesco, A. Varlamov, and D. Embriaco, Phys. Rev. B **65**, 144523 (2002).
- [15] C.A.R. Sá de Melo, M. Randeria, J.R. Engelbrecht, Phys. Rev. Lett. **71**, 3202 (1993). See also M. Randeria, in *Bose-Einstein Condensation*, ed. A. Griffin, D.W. Snoke, and S. Stringari (Cambridge University Press, Cambridge), 1995, and references therein.
- [16] V.J. Emery and S.A. Kivelson, Nature **374**, 434 (1995).
- [17] B. Batlogg and V.J. Emery, Nature **382**, 20 (1996).
- [18] J. Schmalian, D. Pines, and B. Stojković, Phys. Rev. B **60**, 667 (1999).

- [19] J. Bouvier and J. Bok, in *The gap symmetry and fluctuations in high- $T_C$  superconductors*, ed. J. Bok, G. Deutscher, D. Pavuna, and S.A. Wolf (NATO-ASI series, Plenum), 1998, p. 37.
- [20] P.W. Anderson, *The theory of superconductivity in the high- $T_C$  cuprates* (Princeton University Press, Princeton), 1997, and references therein.
- [21] V.B. Geshkenbein, L.B. Ioffe, and A.I. Larkin, Phys. Rev. B **55**, 3173 (1997).
- [22] X.J. Chen, H.Q. Lin, and C.D. Gong, Phys. Rev. B **61**, 9782 (2000).
- [23] J.-P. Locquet, Y. Jaccard, A. Cretton, E.J. Williams, F. Arrouy, E. Mächler, T. Schneider, Ø. Fischer, P. Martinoli, Phys. Rev. B **54**, 7481 (1996).
- [24] H. Sato and M. Naito, Physica C **274**, 221 (1997); H. Sato, A. Tsukada, M. Naito, A. Matsuda, Phys. Rev. B **61**, 12447 (2000).
- [25] I. Bozovic, G. Logvenov, I. Belca, B. Narimbetov, and I. Sveklo, Phys. Rev. Lett. **89**, 107001 (2002).
- [26] H.L. Kao, J. Kwo, R.M. Fleming, M. Hong, and J.P. Manaerts, Appl. Phys. Lett. **59**, 2748 (1991).
- [27] For a review of the influence of the inhomogeneities on the measurements of superconducting fluctuations, see F. Vidal, J.A. Veira, J. Maza, J. Mosqueira, and C. Carballeira, in *Materials Science, Fundamental properties and Future Electronic Applications of High  $T_C$  Superconductors*, ed. S.L. Drechsler and T.M. Mishonov (Kluwer, Dordrecht), 2001, p. 289. See also the references therein.
- [28] J.A. Veira and F. Vidal, Phys. Rev. B **42**, R8748 (1990).
- [29] M.V. Ramallo, A. Pomar, and F. Vidal, Phys. Rev. B **54**, 4341 (1996), and references therein.
- [30] S.K. Yip, Phys. Rev. B **41**, 2612 (1990).
- [31] M.T. Béal-Monod and K. Maki, Europhys. Lett. **33**, 309 (1996).
- [32] C. Carballeira, S.R. Currás, J. Viña, J.A. Veira, M.V. Ramallo, and F. Vidal, Phys. Rev. B **63**, 144515 (2001).
- [33] J. Viña, J.A. Campá, C. Carballeira, S.R. Currás, A. Maignan, M.V. Ramallo, I. Rasines, J.A. Veira, P. Wagner, and F. Vidal, Phys. Rev. B **65**, 212509 (2002).
- [34] F. Vidal, C. Carballeira, S.R. Currás, J. Mosqueira, M.V. Ramallo, J.A. Veira, and J. Viña, Europhys. Lett. **59**, 754 (2002) (cond-mat/0112486). A natural extension of the ideas summarized in this reference is provided by the superconducting fluctuations in the so-called high reduced-magnetic field regime, when  $h \equiv H/H_{c2}(0)$

becomes of the order of unity, where  $H$  is the applied magnetic field and  $H_{c2}(0)$  the upper critical field GL amplitude. In this case, the characteristic length of the superconducting wave function becomes of the order of the so-called magnetic length,  $\ell_H = \xi(0)h^{-1/2}$ . Therefore, the decrease of  $\ell_H$  as  $h$  increases will be also bounded by the limitations imposed by the uncertainty principle to the shrinkage of the superconducting wave function, *i.e.*, by the condition  $\ell_H \gtrsim \tilde{c}\xi_0$ , where  $\tilde{c}$  will be a cutoff constant of the order of unity. This directly leads to a reduced magnetic field,  $h^C$ , given by  $\ell_H(h^C) = \tilde{c}\xi_0$ , above which *all* superconducting fluctuations vanish. In the clean BCS limit  $\xi(0) = 0.74\xi_0$  and therefore  $h^C \simeq 0.6/\tilde{c}^2$ .

- [35] A. Gauzzi and D. Pavuna, Phys. Rev. B **51**, 15420 (1995).
- [36] Expressions for the Levanyuk-Ginzburg reduced-temperature,  $\varepsilon_{LG}$ , in layered superconductors were calculated in M.V. Ramallo and F. Vidal, Europhys. Lett. **39**, 177 (1997). Due to the ambiguities in the background subtraction and in the  $T_C$  determination, to discriminate between the 3DXY and GGL behaviors in the paraconductivity data it is necessary to supplement their analysis with those of other superconducting fluctuation-induced observables. This was made for the case of the optimally-doped YBCO $x$  by Ramallo and coworkers in Ref. [29]. These analyses of high-quality data obtained in single crystals, not appreciably affected by stoichiometric and structural inhomogeneities, confirmed that in the  $\varepsilon \gtrsim 10^{-2}$  region the superconducting fluctuations behave as mean-field-like, whereas for  $\varepsilon \lesssim 10^{-2}$  they follow the 3DXY predictions, in agreement then with the estimates based on the Levanyuk-Ginzburg criterion [see also M.V. Ramallo, C. Carballeira, and F. Vidal, Physica C **341-348**, 173 (2000)].
- [37] J. Mosqueira, C. Carballeira, and F. Vidal, Phys. Rev. Lett. **87**, 167009 (2001).
- [38] In fact, this estimate is expected to be crudely correct also in moderately dirty BCS superconductors (when  $\ell \lesssim \xi_0$ ,  $\ell$  being the mean free path of the normal carriers) because both the GL coherence length amplitude and the actual superconducting coherence length at  $T = 0$  K will be affected by impurities to a similar extent [see, *e.g.*, P.G. de Gennes, *Superconductivity of Metals and Alloys* (W.A. Benjamin, New York), 1966, § 7-2].
- [39] M.V. Ramallo, C. Carballeira, J. Viña, J.A. Veira, T. Mishonov, D. Pavuna, and F. Vidal, Europhys. Lett. **48**, 79 (1999).
- [40] C. Carballeira, J. Mosqueira, A. Revcolevschi, and F. Vidal, Phys. Rev. Lett. **84**, 3157 (2000); Physica C **384**, 185 (2003).
- [41] Y. Nakamura and S. Uchida, Phys. Rev. B **46**, 5841 (1992).
- [42] T. Shibauchi, H. Kitano, K. Uchinokura, A. Maeda, T. Kimura, and K. Kishio, Phys. Rev. Lett. **72**, 2263 (1994).

- [43] J.M. Kosterlitz and D.J. Thouless, *J. Phys. C* **6**, 1181 (1973).
- [44] See, *e.g.*, C.M. Varma, *Phys. Rev. Lett.* **83**, 3538 (1999); see also, C. Panagopoulos, J.L. Tallon, B.D. Rainford, T. Xiang, J.R. Cooper, and C.A. Scott, *Phys. Rev. B* **66**, 064501 (2002), and references therein.
- [45] M.L. Horbach, F.L.J. Vos, and W. van Saarloos, *Phys. Rev. B* **49**, 3539 (1994).
- [46] H.L. Kao, J. Kwo, H. Takagi, and B. Batlogg, *Phys. Rev. B* **48**, 9925 (1993).

x	thickness (nm)	$\rho_{ab}$ (250K) ( $\mu\Omega\text{cm}$ )	$T_{CI}$ ( $T_{CI}^- - T_{CI}^+$ ) (K)	$\xi_c(0)$ ( $\text{\AA}$ )	$\epsilon^C$
0.10	130	1200	21.1 (20.3-22.3)	0.9 (0.7-1.2)	0.8 (0.4-1.1)
0.12	150	830	23.8 (22.6-25.5)	0.8 (0.7-1.2)	0.7 (0.4-1.0)
0.15	150	580	27.2 (26.2-28.3)	0.9 (0.7-1.2)	0.8 (0.4-1.1)
0.20	150	310	26.3 (25.1-27.7)	0.5 (0-0.9)	0.8 (0.4-1.1)
0.25	120	230	14.8 (14.0-15.9)	0 (0-0.5)	0.7 (0.4-0.9)

Table I:

Summary of the main parameters of the LSxCO thin films studied in this work. The  $T_{CI}$ ,  $T_{CI}^-$  and  $T_{CI}^+$  temperatures are represented in Fig. 3. The  $\xi_c(0)$  and  $\epsilon^C$  main values are the ones resulting from the  $\Delta\sigma_{ab}(\epsilon)$  fits presented in Fig. 5. Their uncertainties result from considering different normal-state backgrounds (see Fig. 9 and main text).

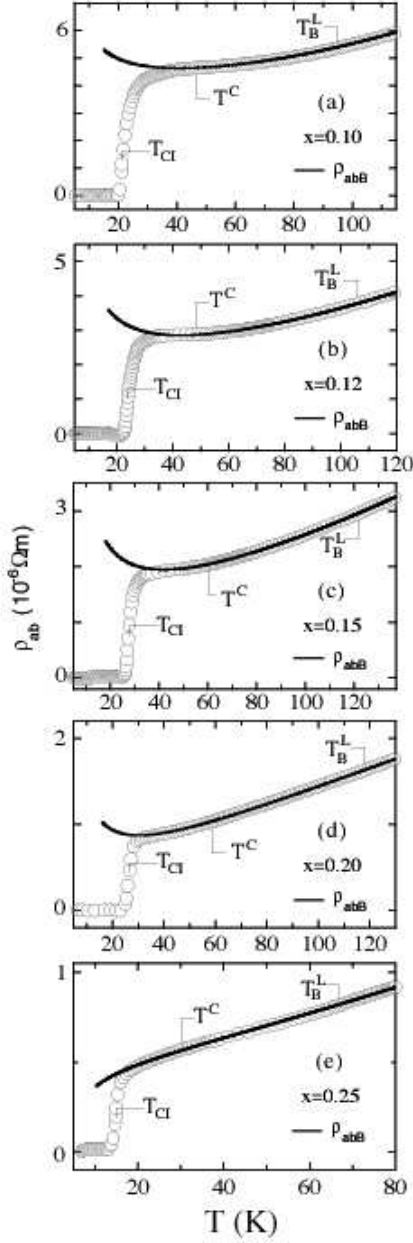


Figure 1:

The in-plane resistivity measured in this work (circles) in various  $LSxCO$  thin films with different doping levels  $x$ . We also indicate (solid line) the normal-state background of each film, obtained by using the procedure indicated in the main text. The temperature  $T_B^L$  corresponds to the lower limit of the fitting region used to extract such background. The temperature  $T^C$  is the one at which the background and the experimental data first deviate from each other (*i.e.*, the temperature above which fluctuation effects are no longer observed). Note that  $T^C$  is located well below  $T_B^L$  (see also main text for details).  $T_{CI}$  is the temperature where  $d\rho_{ab}/dT$  is maximum, that is expected to be close to  $T_C$ , the mean-field normal-superconductor transition temperature.

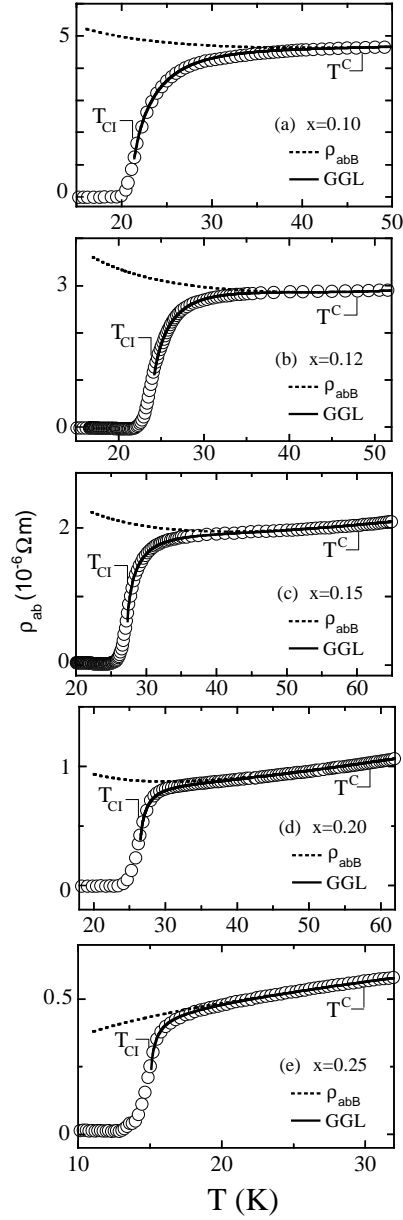


Figure 2:

Amplification of the view in Fig. 1 to better appreciate the range of temperatures where the fluctuation effects above the transition are observed. The dashed line corresponds to the normal-state background and the solid line corresponds to the theoretical  $\rho_{ab}(T)$  obtained by using in Eq. (1) such a background and the best fit by the GGL theory extended to high reduced-temperatures through its regularization with a so-called “total-energy” cutoff which takes into account the quantum localization energy.

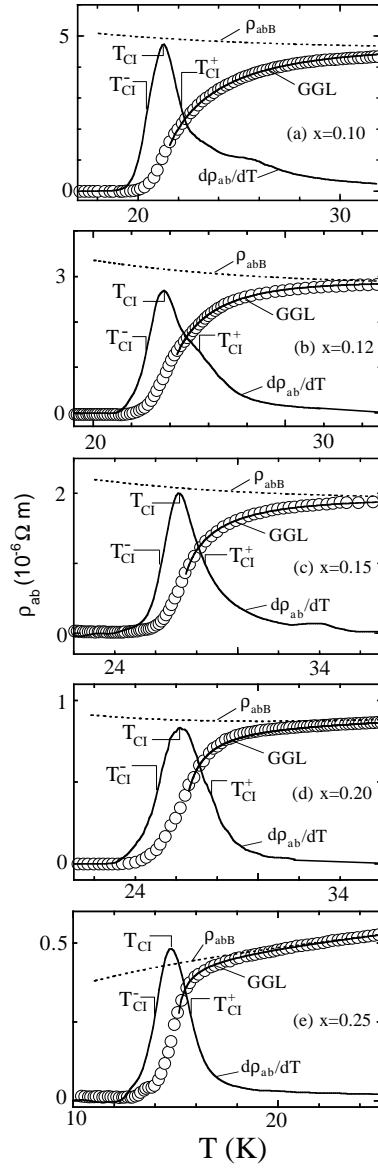


Figure 3:

Scoop of Figs. 1 and 2 to better appreciate the region closer to  $T_{CI}$ , the temperature where  $d\rho_{ab}/dT$  is maximum. Such a  $d\rho_{ab}/dT$  peak is also plotted, in arbitrary units (as a solid line). The temperatures  $T_{CI}^-$  and  $T_{CI}^+$  correspond to the half-maximum boundaries of such a peak. The circles are the experimental  $\rho_{ab}(T)$  data, the dashed line is the normal-state background, and the solid line following the data is the  $\rho_{ab}(T)$  resulting from such a background and the “extended” GGL theory with a total-energy cutoff.

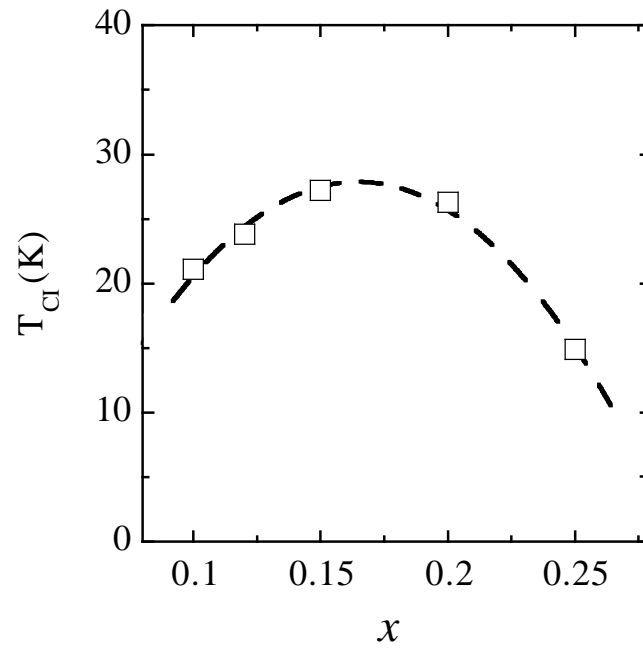


Figure 4:

The temperature  $T_{CI}$  where it is located the inflexion point of the  $\rho_{ab}(T)$  transition (see Figs. 2 and 3) versus the Sr-content  $x$  in the  $LSxCO$  films measured in this work. The dashed line is a parabolic fit which serves as a guide for the eyes. Note that both the absolute values and the doping dependence of such  $T_{CI}$  is in fairly good agreement with the one well established [1, 4, 23, 24, 26, 33] for the critical temperature of  $LSxCO$  films grown on  $(100)SrTiO_3$  substrates and with similar thickness.

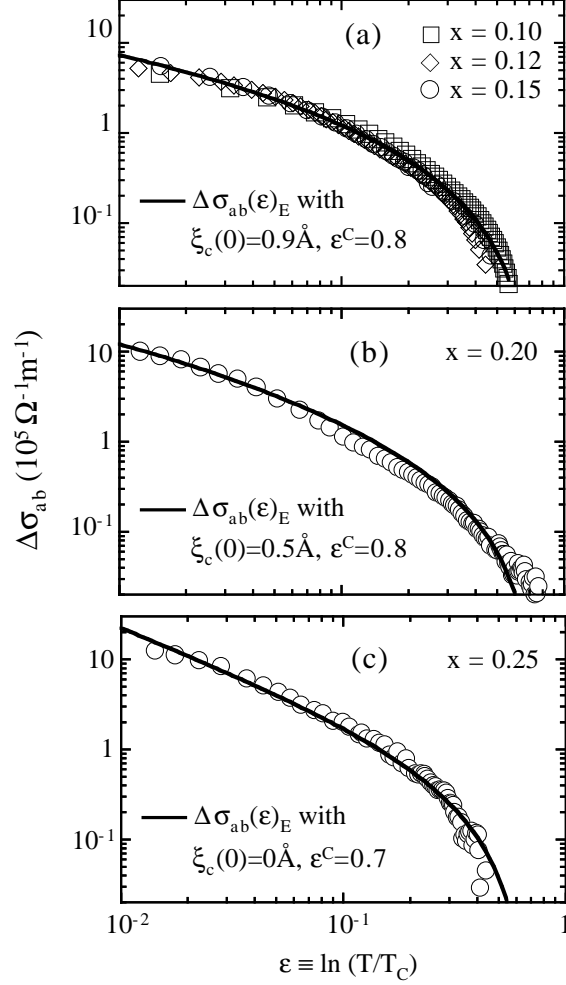


Figure 5:

Comparison between the “extended” GGL expressions for  $\Delta\sigma_{ab}(\varepsilon)$  using a total-energy cutoff [solid lines, Eq.(8)] and the experimental curves of the in-plane paraconductivity versus reduced-temperature in the  $LSxCO$  films measured in this work (circles). In these comparisons we use  $T_{CI}$  as critical temperature (see main text). As it can be seen in Fig. (a), the experimental  $\Delta\sigma_{ab}(\varepsilon)$  curves for the underdoped and optimally-doped  $LSxCO$  films are essentially coincident. The corresponding  $\Delta\sigma_{ab}(\varepsilon)$  for the overdoped films [Figs. (b) and (c)] show a moderate increase as  $x$  increases. The GGL fits are able to account for such data in all the studied  $\varepsilon$ -range, including also the disappearance of observable fluctuation effects at high reduced-temperatures. See main text for details.

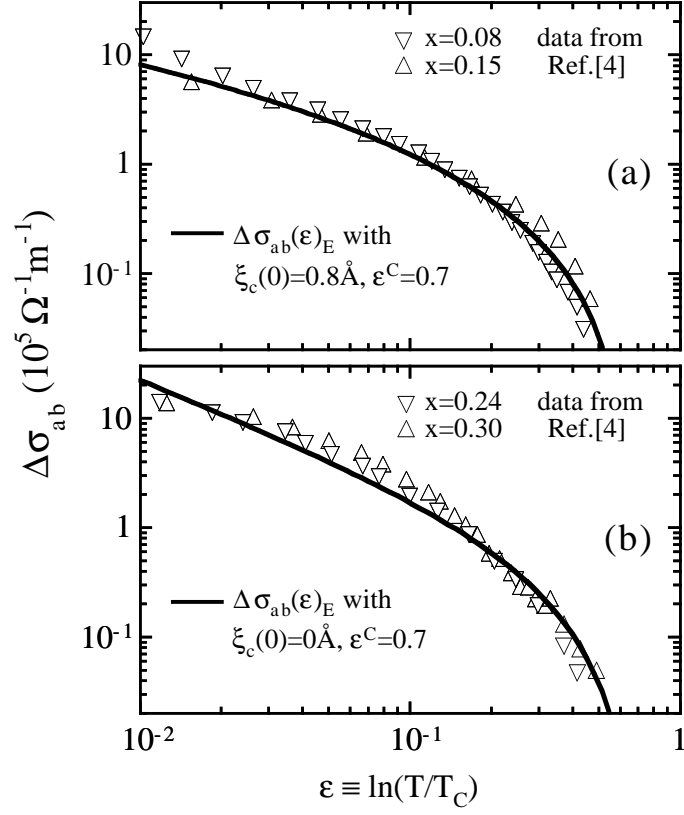


Figure 6:

Some examples of the in-plane paraconductivity versus reduced-temperature curves that result from applying to the  $\rho_{ab}(T)$  data measured by Suzuki and Hikita [4] in  $LSxCO$  films the same analyses as we have applied to our present measurements. The solid lines correspond to the fits using the “extended” GGL approach with a total-energy cutoff. Such fits fully confirm the results found with our own measurements (compare, *e.g.*, with Fig. 5).

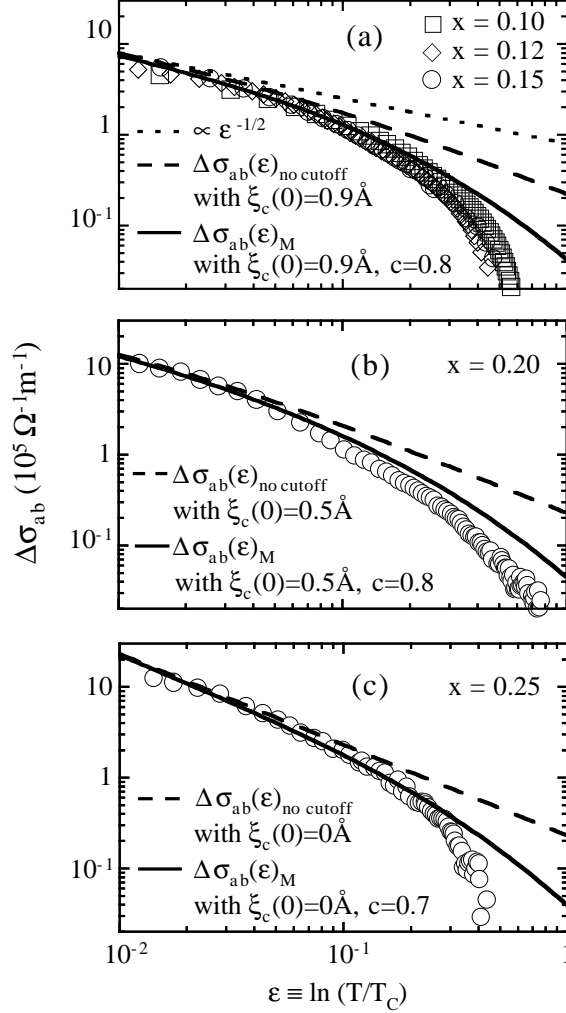


Figure 7:

Comparison between the same experimental curves as in Fig. 5 and the paraconductivity expressions without any cutoff [dashed lines, Eq.(15)] and with the momentum or kinetic-energy cutoff [continuous lines, Eq.(11)]. In performing these comparisons, we have used the same values for  $\xi_c(0)$  and the cutoff constant as in Fig. 5. In Fig. 7(a) we also indicate the low- $\varepsilon$  asymptotic  $\Delta\sigma_{ab}(\varepsilon) \propto \varepsilon^{-1/2}$ , which would correspond to the 3D limit without any cutoff. The dashed line in Fig. 7(c) corresponds also to  $\Delta\sigma_{ab}(\varepsilon) \propto \varepsilon^{-1}$ , *i.e.*, the 2D limit without any cutoff. The  $\varepsilon \sim 10^{-2}$  paraconductivity of the  $x = 0.20$  film does not follow any of such dimensionality limit cases, but lies instead in the dimensional crossover regime. Note that the momentum or kinetic-energy cutoff expressions are able to explain the experimental paraconductivity in a lower  $\varepsilon$ -range than the total-energy cutoff (up to at most  $\varepsilon \simeq 0.3$ ). The expressions without any cutoff explain the data in a even more limited  $\varepsilon$ -range,  $\varepsilon \lesssim 0.1$ .

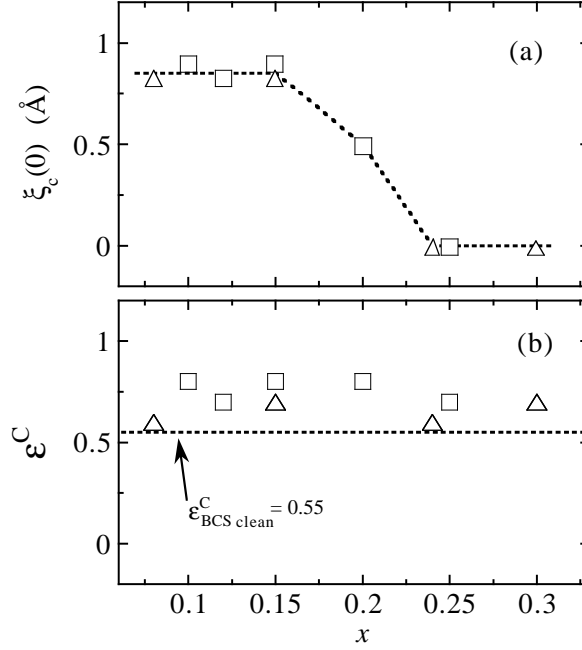


Figure 8:

The values of the  $c$ -direction coherence length GL amplitude,  $\xi_c(0)$ , and of the total-energy cutoff amplitude,  $\varepsilon^C$ , providing the best fit to the  $\Delta\sigma_{ab}(\varepsilon)$  data (see Figs. 5 and 6), represented versus the Sr-content (*i.e.*, hole doping)  $x$ . The squares correspond to the LS $x$ CO films measured in the present work, while the triangles correspond to the films measured by Suzuki and Hikita [4] analyzed in Fig. 6. As it can be easily seen in Fig.(a),  $\xi_c(0)$  is constant, well within the experimental uncertainties, for the underdoped ( $x < 0.15$ ) and optimally-doped ( $x = 0.15$ ) films. When entering in the overdoped range ( $x > 0.15$ ),  $\xi_c(0)$  decreases up to being negligible [ $\xi_c(0) \simeq 0$  Å] at about  $x \simeq 0.25$  and above. The dashed line in this Fig.(a) is a guide for the eyes. Figure (b) illustrates that the cutoff amplitude  $\varepsilon^C$  is found to be, within the experimental uncertainties, constant for all doping levels. The continuous line in this Fig.(b) is the crude estimate  $\varepsilon_{\text{BCS clean}}^C \simeq 0.6$  that can be obtained by using the BCS theory in the clean limit (see main text). Note that the  $\varepsilon^C$  values shown in this figure are somewhat above such an estimate. However, such differences cannot be taken as significant, in view of the error bars of  $\varepsilon^C$  in our  $\Delta\sigma_{ab}(\varepsilon)$  analyses (see main text and Table I).

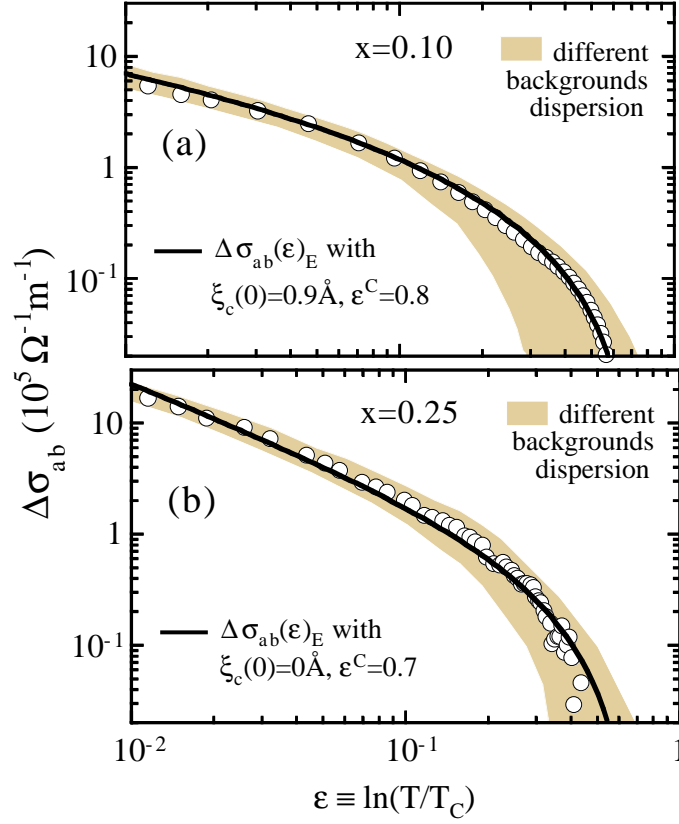


Figure 9:

Influence of the use of different normal-state backgrounds in the experimental  $\Delta\sigma_{ab}(\varepsilon)$  curves of (a) the  $x = 0.10$  film and (b) the  $x = 0.25$  film measured in this work. Such a background uncertainty is discussed in detail in the main text. The corresponding uncertainties in  $\varepsilon^C$  and  $\xi_c(0)$  are summarized in Table I for all the films measured in this work.

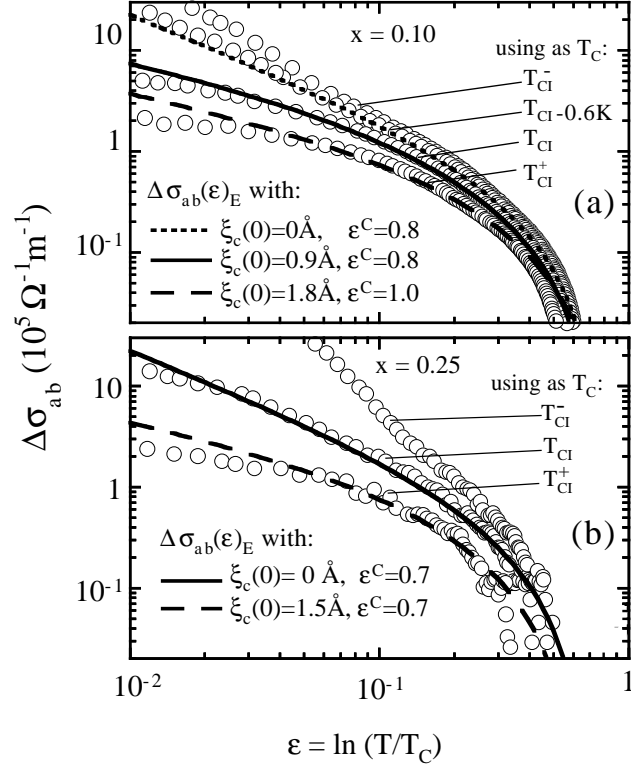


Figure 10:

Influence of the choice of  $T_C$  in the experimental  $\Delta\sigma_{ab}(\varepsilon)$  curves and GGL fits, for (a) the  $x = 0.10$  film and (b) the  $x = 0.25$  film measured in this work. The  $T_C$  choice varies mainly the  $\Delta\sigma_{ab}(\varepsilon)$  slope in the  $\varepsilon \lesssim 0.1$  region. As easily visible in these figures, using  $T_C$ 's below  $T_{CI}$  does not allow to fit the data with Eq.(8) for all the doping levels, and  $T_C$ 's above  $T_{CI}$  produce poorer fits than  $T_{CI}$ . The other underdoped and optimally-doped films studied in this work produce curves similar to the  $x = 0.10$  ones, and the  $x = 0.20$  film produces results intermediate between those of (a) and (b).